Hindawi
Discrete Dynamics in Nature and Society
Volume 2019, Article ID 1452380, 12 pages
https://doi.org/10.1155/2019/1452380

Research Article

Robust Nonfragile H_∞ Control of Lateral Semiactive Suspension of Rail Vehicles

Jianjun Meng,[1,2,3] **Ruxun Xu**,[1,2] **and Decang Li**[1,2]

[1] *Mechatronics T&R Institute, Lanzhou Jiaotong University, Lanzhou, 730070, China*
[2] *School of Mechatronic Engineering, Lanzhou Jiaotong University, Lanzhou, 730070, China*
[3] *Engineering Technology Center for Informatization of Logistics & Transport Equipment, Lanzhou, 730070, China*

Correspondence should be addressed to Jianjun Meng; mengjj1966@163.com

Received 6 May 2019; Accepted 2 July 2019; Published 24 July 2019

Academic Editor: Xiaohua Ding

This paper focuses on the riding comfort of railway vehicle. A nonfragile control strategy is proposed based on robust theory for semiactive suspension system. First, the rail vehicle dynamic model was simplified reasonably, the control model of rail vehicle train lateral semiactive suspension was built, which involved lateral-moving, head-shaking, and side-rolling of the vehicle body and the lateral-moving of the two bogies, and the robust nonfragile H_∞ control of head-shaking and side-rolling were designed, respectively. Then the H_∞ norm was used to reflect riding comfort; the sufficient conditions for the existence of robust nonfragile H_∞ control were developed based on linear matrix inequality (LMI) approach. The design of a robust nonfragile H_∞ control with gain perturbation was changed into an optimization issue with linear inequality constraint and a linear objective function. And then the damping effect of the robust nonfragile H_∞ controller was evaluated, the wavelet packet analysis theory was used to decompose and reconstruct the acceleration signal, the fragility of the controller was analyzed, and the theory of mathematical statistics was adopted to analyze the influence of robust nonfragile H_∞ controller on the probability distribution of vibration acceleration. Finally, the simulation results show that the proposed control strategy can ensure the riding comfort of railway vehicle efficiently and has a comparatively strong nonfragility.

1. Introduction

Remarkable achievements have been made in China's high-speed train in recent years. In the course of high-speed operation, due to the unsmooth track, transverse vibration is inevitable. How to effectively suppress the transverse vibration of orbital vehicle is a hot research topic in the field of train control. Compared with the traditional passive suspension system, semiactive suspension system can repress vehicle's vibration effectively and make the dynamic performance of vehicle better [1, 2]. In order to achieve these control objectives, it is necessary to design an efficient and reliable control algorithm for semiactive suspension system. Hsieh C. Y. raised a regenerative ceiling damping control strategy and got remarkable damping effect with the energy consumption and riding comfort of the semiactive suspension system considered [3]. Guo Jin raised a new semiactive control strategy based on the ceiling damping control through restraining the lateral vibration of the bogie and wheel set to reduce the derailment factor of railway vehicles [4]. Chen Shian and his team adopted LQG arithmetic and gave a systematic research to the optimization design of the suspension system, in order to raise vehicle's riding comfort and reduce the manufacturing and operating costs [5]. Yang junghua realized the suspension system's self-adaptive control by designing excitation current properly and proved feasibility of the control strategy by experiment [6]. Guo Konghui took overall consideration of the ceiling damping and floor damping and raised a mixed damping control that can improve trains' vibration performance effectively [7]. Liu Hongyou made experiment and simulation on continuous adjustable damping semiactive suspension, with the damping effect of the suspension being analyzed in detail [8]. Li Guangjun set up the model of 17-DOF and introduced the variable universe fuzzy control theory and applied it to the design of semiactive suspension [9]. Li Zhongji and his team constructed the

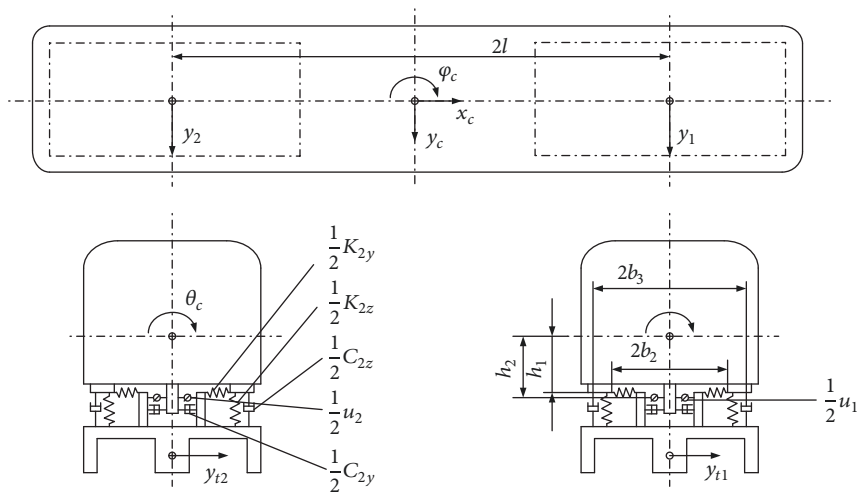

Figure 1: The control model for lateral semiactive suspension of rail vehicles.

model of magnet or heliacal damper and designed a fuzzy controller for semiactive suspension system and proved the effectiveness of the semiactive suspension system by simulation [10].

The rail vehicle under the actual running state is a very complex multicoupled system and is influenced by many uncertain factors; it is difficult to establish its exact mathematical model. Robust H_∞ control can overcome the defects of the traditional control strategy effectively and keep system's stability and restrain the vehicle's vibration effectively when uncertain factors arise in vehicle's suspension system. However, unignorably, the accuracy of robust controller execution has a great influence on its implementation. In the actual running state, frequent parameter perturbations are found in the controller. Therefore, it is necessary to comprehensively analyze the uncertainty of the controller when designing a semiactive suspension robust controller [11]. So that the stability of the controller can have a strong tolerance to the perturbation of the parameters that is to ensure that the controller is nonfragile [12–15].

In this paper, the robust nonfragile H_∞ control considering the perturbation of the controller is studied, which can simplify the lateral dynamic model of rail vehicle and establish the control model of lateral semiactive suspension of rail vehicle. The existence condition of the robust nonfragile H_∞ controller for the movement of the moving body and the rolling motion of the vehicle is derived by using the linear matrix inequality. Meanwhile, rail vehicle dynamic model is set up by using ADAMS/Rail. Simulations to passive control and the method mentioned in this paper in time domain and frequency domain are conducted, respectively.

2. Dynamic Model of Semiactive Lateral Suspension of Railway Vehicles

In practical application, it is of paramount importance to set up a lower level controller to facilitate real-time control. The dynamics model used to design controller needs to adequately reflect the effects of the semiactive suspension on the train, but without regard to the details of the train. The rail vehicle's lateral dynamic simulative model, which has taken into consideration the complicated interaction force among wheel sets and the characteristics of high DOF, is of great necessity to be simplified. The controller designed in this paper is mainly used to restrain vehicle body's lateral vibration, focusing on the influence of the central suspension on the lateral vibration of the vehicle body but taking no consideration of the axle box suspension structure, etc. The simplified rail vehicle lateral semiactive suspension control model is shown as Figure 1.

Based on Newton's second law, the dynamic equation of transverse vibration of urban rail train body can be obtained from Figure 1.

Vehicle body lateral movement:

$$\begin{aligned} M_C\ddot{y}_c &+ K_{2y}\left(y_c + l\varphi_c - h_1\theta_c - y_{t1}\right) \\ &+ C_{2y}\left(\dot{y}_c + l\dot{\varphi}_c - h_2\dot{\theta}_c - \dot{y}_{t1}\right) \\ &+ K_{2y}\left(y_c + l\varphi_c - h_1\theta_c - y_{t2}\right) \\ &+ C_{2y}\left(\dot{y}_c - l\dot{\varphi}_c - h_2\dot{\theta}_c - \dot{y}_{t2}\right) = u_1 + u_2 \end{aligned} \tag{1}$$

Vehicle body shaking movement:

$$\begin{aligned} J_{cz}\ddot{\phi}_c &+ K_{2y}l\left(y_c + l\phi_c - h_1\theta_c - y_{t1}\right) \\ &+ C_{2y}l\left(\dot{y}_c + l\dot{\phi}_c - h_2\dot{\theta}_c - \dot{y}_{t1}\right) \\ &- K_{2y}l\left(y_c - l\phi_c - h_1\theta_c - y_{t2}\right) \\ &- C_{2y}l\left(\dot{y}_c - l\dot{\phi}_c - h_2\dot{\theta}_c - \dot{y}_{t2}\right) = u_1 l - u_2 l \end{aligned} \tag{2}$$

Vehicle body side-rolling movement:

$$\begin{aligned} J_{cx}\ddot{\theta}_c &- K_{2y}h_1\left(y_c + l\phi_c - h_1\theta_c - y_{t1}\right) \\ &- C_{2y}h_2\left(\dot{y}_c + l\dot{\phi}_c - h_2\dot{\theta}_c - \dot{y}_{t1}\right) \\ &- K_{2y}h_1\left(y_c - l\phi_c - h_1\theta_c - y_{t2}\right) \end{aligned}$$

$$-C_{2y}h_2\left(\dot{y}_c - l\dot{\phi}_c - h_2\dot{\theta}_c - \dot{y}_{t2}\right) + 2K_{2z}b_2^2\theta_c + 2C_{2z}b_3^2\dot{\theta}_c = -u_1h_2 - u_2h_2 \tag{3}$$

In the equation, M_c is the quality of vehicle body, J_{cz} is the rotational inertia of vehicle body shaking movement, J_{cx} is rotational inertia of vehicle body side-rolling movement, y_c is vehicle lateral motion, ϕ_c is the vehicle shaking angle motion, θ_c is vehicle sidewinder angle, y_{t1} and y_{t2} are lateral displacements of front and rear bogies, respectively, h_1 is the vertical distance from vehicle core to the secondary level spring connection point, h_2 is the vertical distance from vehicle core to the secondary level spring lateral damper, l is the half of distance, b_2 is the half of lateral span of the secondary level vertical spring, b_3 is the half of lateral span of the secondary level vertical shock absorber, K_{2y} is the double lateral stiffness coefficient of the secondary level suspension, C_{2y} is the double lateral damping coefficient of the secondary level suspension, K_{2z} is the double vertical stiffness coefficient of the secondary level suspension, C_{2z} is the double vertical damping coefficient of the secondary level suspension, and u_1 and u_2 are the controlling forces which the lateral actuator installed on the front and rear bogies exerts on vehicle body, respectively.

The y_1 and y_2 are defined as the lateral motion before and rear ends of vehicle body and the joint of semiactive suspension, the lateral motion (y_c) and shaking angle motion (ϕ_c), respectively, are

$$y_c = \frac{(y_1 + y_2)}{2} \tag{4}$$

$$\phi_c = \frac{(y_1 - y_2)}{2l} \tag{5}$$

Simplifying (1)~(3) we can get

$$M_c\ddot{y}_c + 2K_{2y}\left(y_c - h_1\theta_c\right) - K_{2y}\left(y_{t1} + y_{t2}\right) + 2C_{2y}\left(\dot{y}_c - h_2\dot{\theta}_c\right) - C_{2y}\left(\dot{y}_{t1} + \dot{y}_{t2}\right) = u_1 + u_2 \tag{6}$$

$$J_{cz}\ddot{\phi}_c + 2K_{2y}l^2\phi_c - K_{2y}l\left(y_{t1} - y_{t2}\right) + 2C_{2y}l^2\dot{\phi}_c - C_{2y}l\left(\dot{y}_{t1} - \dot{y}_{t2}\right) = u_1l - u_2l \tag{7}$$

$$J_{cx}\ddot{\theta}_c - 2K_{2y}h_1y_c + 2\left(K_{2y}h_1^2 + K_{2z}b_2^2\right)\theta_c + K_{2y}h_1\left(y_{t1} + y_{t2}\right) - 2C_{2y}h_2\dot{y}_c + 2\left(C_{2y}h_2^2 + C_{2z}b_3^2\right)\dot{\theta}_c + C_{2y}h_2\left(\dot{y}_{t1} + \dot{y}_{t2}\right) = -u_1h_2 - u_2h_2 \tag{8}$$

In the above formula, it can be found that the shaking motion of the vehicle and the rolling motion are weakly coupled, so the controllers for these two movements can be designed separately to make the controller more simplified.

3. The Design of Robust Nonfragile H_∞ Controller

3.1. Shaking Motion Robust Nonfragile H_∞ Controller. For the vehicle body shaking movement, defining $y_{Yc} = (y_1 - y_2)/2$, $y_{Yt} = (y_{t1} - y_{t2})/2$, $\Delta y_Y = y_{Yc} - y_{Yt}$, $u_Y = (u_1 - u_2)/2$. Define $x_Y = [\dot{y}_{Yc}, \Delta y_Y]^T$ as controller's state vector. In order to restrain vehicle lateral vibration and adjust the size of control force in the suitable section effectively, selecting evaluating output as $z_Y = [\ddot{y}_{Yc}, u_Y]^T$; selecting the accelerated speed ($y_Y = x_Y$) sign that is easier to measure in the actual situation as measuring output, disturbance input is $w_Y = \dot{y}_{Yt}$. The state equation of vehicle shaking motion can be established by (5) and (7):

$$\begin{aligned} \dot{x}_Y(t) &= A_Yx_Y(t) + B_Yu_y(t) + B_{Y1}w_Y(t) \\ z_Y(t) &= C_Yx_Y(t) + D_Yu_y(t) + D_{Y1}w_Y(t) \\ y_Y(t) &= x_Y(t) \end{aligned} \tag{9}$$

In the equation,

$$\begin{aligned} A_Y &= \begin{bmatrix} -\dfrac{2C_{2y}l^2}{J_{cz}} & -\dfrac{2K_{2y}l^2}{J_{cz}} \\ 1 & 0 \end{bmatrix} \\ B_Y &= \begin{bmatrix} \dfrac{2C_{2y}l^2}{J_{cz}} \\ -1 \end{bmatrix} \\ B_{Y1} &= \begin{bmatrix} \dfrac{l^2}{J_{cz}} \\ 0 \end{bmatrix} \\ C_Y &= \begin{bmatrix} -\dfrac{2C_{2y}l^2}{J_{cz}} & -\dfrac{2K_{2y}l^2}{J_{cz}} \\ 0 & 0 \end{bmatrix} \\ D_Y &= \begin{bmatrix} \dfrac{2C_{2y}l^2}{J_{cz}} \\ 0 \end{bmatrix} \\ D_{Y1} &= \begin{bmatrix} \dfrac{l^2}{J_{cz}} \\ 1 \end{bmatrix} \end{aligned} \tag{10}$$

Consider the following fragile state feedback control:

$$u_Y(t) = \left(K_Y + \Delta K_Y\right)y_Y(t) = \left(K_Y + \Delta K_Y\right)x_Y(t) \tag{11}$$

In the equation, K_Y is the controller gain, ΔK_Y is the additive controller gain involved dynamic matrix, H_Y and E_Y are the constant matrixes with suitable dimension, and F_Y is the unknown matrix with Lebesgue that is measurable and satisfy additional gain perturbation:

$$\begin{aligned} \Delta K_Y &= H_YF_YE_Y, \\ {F_Y}^TF_Y &\le I \end{aligned} \tag{12}$$

Making $A_{Ycl} = A_Y + B_Y(K_Y + \Delta K_Y)$, $C_{Ycl} = C_Y + D_Y(K_Y + \Delta K_Y)$, then relevant closed-loop system is

$$\begin{aligned} \dot{x}(t) &= A_{Ycl}x(t) + B_{Y1}w(t) \\ z(t) &= C_{Ycl}x(t) + D_{Y1}w(t) \end{aligned} \tag{13}$$

Aiming at vehicle shaking motion (9) and positive number given, $\gamma > 0$ design form as (11) robust nonfragile H_∞ controller, it makes closed-loop system (13) asymptotically stable, and the outside disturb an w_Y and the transmit function T_{wz} of the evaluation output z_Y satisfy

$$\left\|T_{wz}(s)\right\|_\infty = \left\|C_{Ycl}\left(sI - A_{Ycl}\right)^{-1} B_{Y1} + D_{Y1}\right\|_\infty < \gamma \tag{14}$$

Finally the rail vehicle lateral vibration is restrained effectively, and the safety and stability of train operation is improved.

Theorem 1 (see [16]). *To system equation (13), assume $\gamma > 0$ is a given constant, then the following conditions are equivalent.*

(1) *System is asymptotically stable, and $\|T_{zw}(s)\|_\infty \le \gamma$;*

(2) *There is a symmetry enfilade matrix $P > 0$ making*

$$\begin{bmatrix} A_{Ycl}^T P + PA_{Ycl} & PB_{Y1} & C_{Ycl}^T \\ B_{Y1}^T P & -\gamma^2 I & D_{Y1}^T \\ C_{Ycl} & D_{Y1} & -I \end{bmatrix} < 0 \tag{15}$$

Lemma 2 (see [16]). *H, F, E are assumed as matrixes of random suitable dimension, $F^T F \ge I$, for random scalar invariant $\varepsilon > 0$, and there is $HFE + E^T F^T H^T \le \varepsilon^{-1} HH^T + \varepsilon E^T E$.*

Theorem 3. *If there are constants $\gamma > 0$, $\varepsilon > 0$, symmetry positive definite matrix X and matrix Y make linear matrix equation (16) established, so there is a robust nonfragile H_∞ controller (17) which makes closed-loop system (13) internal asymptotically stable:*

$$\begin{bmatrix} \Psi & B_{Y1} & \left(C_Y X + D_Y Y\right)^T & B_Y H_Y & XE_Y{}^T \\ * & -\gamma I & D_{Y1}^T & 0 & 0 \\ * & * & -\gamma I & D_Y H_Y & 0 \\ * & * & * & -\varepsilon I & 0 \\ * & * & * & * & -\varepsilon I \end{bmatrix} < 0 \tag{16}$$

$$K_Y = YX^{-1} \tag{17}$$

In (16), $\Psi = XA_Y{}^T + A_Y X + B_Y Y + Y^T B_Y{}^T$, "$*$" expressed as symmetrical item of matrix.

Base on the above-mentioned existence conditions of state feedback controller, setting up the convex optimization problem with LMI in equation constraint and linear target function

$$\begin{aligned} &\min_{s,t.(16)} \gamma \\ &X > 0 \\ &\gamma > 0, \\ &\varepsilon > 0 \end{aligned} \tag{18}$$

By the LMI tool of MATLAB we can get the result of (18); then we can get robust nonfragile H_∞ controller, and when H, F, E are all zero, (18) can be solved and robust regular H_∞ controller can be obtained.

3.2. Side-Rolling Movement Robust Nonfragile H_∞ Controller. To vehicle side-rolling movement, defining $y_{Lc} = (y_1 + y_2)/2$, $y_{Lt} = (y_{t1} + y_{t2})/2$, $\Delta y_L = y_{Lc} - y_{Lt}$, $u_L = (u_1 + u_2)/2$. Choosing $x_L = [\dot{y}_c, \Delta y_L, \dot{\theta}_c, \theta_c]^T$ as side-rolling movement controller's state vector; choosing $Z_L = [\ddot{y}_{Lc}, u_L]^T$ as evaluating output; choosing $y_L = \ddot{y}_{Lc}$ as measuring output; choosing $w_L = \ddot{y}_{Lt}$ as disturbance output. According to (4), (6), and (8) we can set up state function of vehicle side-rolling movement:

$$\begin{aligned} \dot{x}_L(t) &= A_L x_L(t) + B_L u_L(t) + B_{L1} w_L(t) \\ z_L(t) &= C_L x_L(t) + D_L u_L(t) + D_{L1} w_L(t) \\ y_L(t) &= x_L(t) \end{aligned} \tag{19}$$

Among them,

$$A_L = \begin{bmatrix} -\dfrac{2C_{2y}}{M_c} & -\dfrac{2K_{2y}}{M_c} & \dfrac{2C_{2y}h_2}{M_c} & \dfrac{2K_{2y}h_1}{M_c} \\ 1 & 0 & 0 & 0 \\ \dfrac{2C_{2y}h_2}{J_{cx}} & \dfrac{2K_{2y}h_1}{J_{cx}} & \dfrac{2\left(C_{2y}h_2^2 + C_{2z}b_3^2\right)}{J_{cx}} & \dfrac{2\left(K_{2y}h_1^2 + K_{2z}b_2^2\right)}{J_{cx}} \\ 0 & 0 & 1 & 0 \end{bmatrix},$$

$$B_L = \begin{bmatrix} \dfrac{2C_{2y}}{M_c} \\ -1 \\ -\dfrac{2C_{2y}h_2}{J_{cx}} \\ 0 \end{bmatrix},$$

$$B_{L1} = \begin{bmatrix} \frac{2}{M_c} \\ -1 \\ -\frac{2h_2}{J_{cx}} \\ 0 \end{bmatrix},$$

$$C_L = \begin{bmatrix} -\frac{2C_{2y}}{M_c} & -\frac{2K_{2y}}{M_c} & \frac{2C_{2y}h_2}{M_c} & \frac{2K_{2y}h_1}{M_c} \\ 0 & 0 & 0 & 0 \end{bmatrix},$$

$$D_L = \begin{bmatrix} \frac{2C_{2y}}{M_c} \\ 0 \end{bmatrix},$$

$$D_{L1} = \begin{bmatrix} \frac{2}{M_c} \\ 1 \end{bmatrix} \tag{20}$$

Considering the following nonfragile feedback control,

$$u_L(t) = (K_L + \Delta K_L)\, y_L(t) = (K_L + \Delta K_L)\, x_L(t) \tag{21}$$

In the equation, K_L is controller gain, ΔK_L is additional controller perturbation matrix, and the definition of ΔK_L is given in (12).

Making $A_{Lcl} = A_L + B_L(K_L + \Delta K_L)$, $C_{Lcl} = C_L + D_L(K_L + \Delta K_L)$, so the relevant closed-loop system is

$$\begin{aligned} \dot{x}_L(t) &= A_{Lcl}x_L(t) + B_{L1}w_L(t) \\ z_L(t) &= C_{Lcl}x_L(t) + D_{L1}w_L(t) \end{aligned} \tag{22}$$

If constant $\gamma > 0$, $\varepsilon > 0$ exist in (16), symmetry positive definite matrices X and Y make linear matrix in (23) established, so there is a robust nonfragile H_∞ controller (24) making the inside of the closed-loop uncertain system (22) asymptotically stable.

$$\begin{bmatrix} \Psi & PB_{L1} & (C_LX + D_LY)^T & PB_LH_L & E_L^T \\ * & -\gamma I & D_{L1}^T & 0 & 0 \\ * & * & -\gamma I & D_LH_L & 0 \\ * & * & * & -\varepsilon I & 0 \\ * & * & * & * & -\varepsilon I \end{bmatrix} < 0 \tag{23}$$

$$K_L = YX^{-1} \tag{24}$$

In (24) $\Psi = XA_L^T + A_LX + B_LY + Y^TB_L^T$, "$*$" represents the symmetry of the matrix.

According to the above-mentioned existence conditions of state feedback controller, setting up the following convex optimization problem with LMI in equation constraint and linear target function

$$\begin{aligned} &\min_{s,t.(25)} \gamma \\ &X > 0 \\ &\gamma > 0, \\ &\varepsilon > 0 \end{aligned} \tag{25}$$

We can get the result of (25) by the LMI tool of MATLAB and then get robust nonfragile H_∞ controller; meanwhile when H, F, E are all zero, we can solve (25) and get robust regular H_∞ controller.

4. Simulation and Analysis

Setting up a semiactive suspension robust nonfragile H_∞ controller in the MATLAB/SIMULINK and setting up a rail vehicle model by ADAMS/Rail, guiding the model into MATLAB/Simulink environment to conduct joint simulation via a control module, as is shown in Figure 2, "adams_sub" module is the model of rail vehicle, "controller_RP" module is the side-rolling motion robust nonfragile H_∞ controller, "controller_yaw" is the head-shaking motion robust conventional H_∞ controller.

Writing German low-interference rail chart file in ADAMS/Rail, the circuit is a straight line rail, and the operating speed of vehicle is 300km/h. According to document [17], when adopting passive suspension, the lateral damping coefficient of vehicle secondary-level suspension is 26000N · s/m.

4.1. Time Domain Analysis. Figure 3 is the lateral vibration accelerated speed time-domain plot in passive suspension and robust nonfragile H_∞ controller situation. Table 1 lists

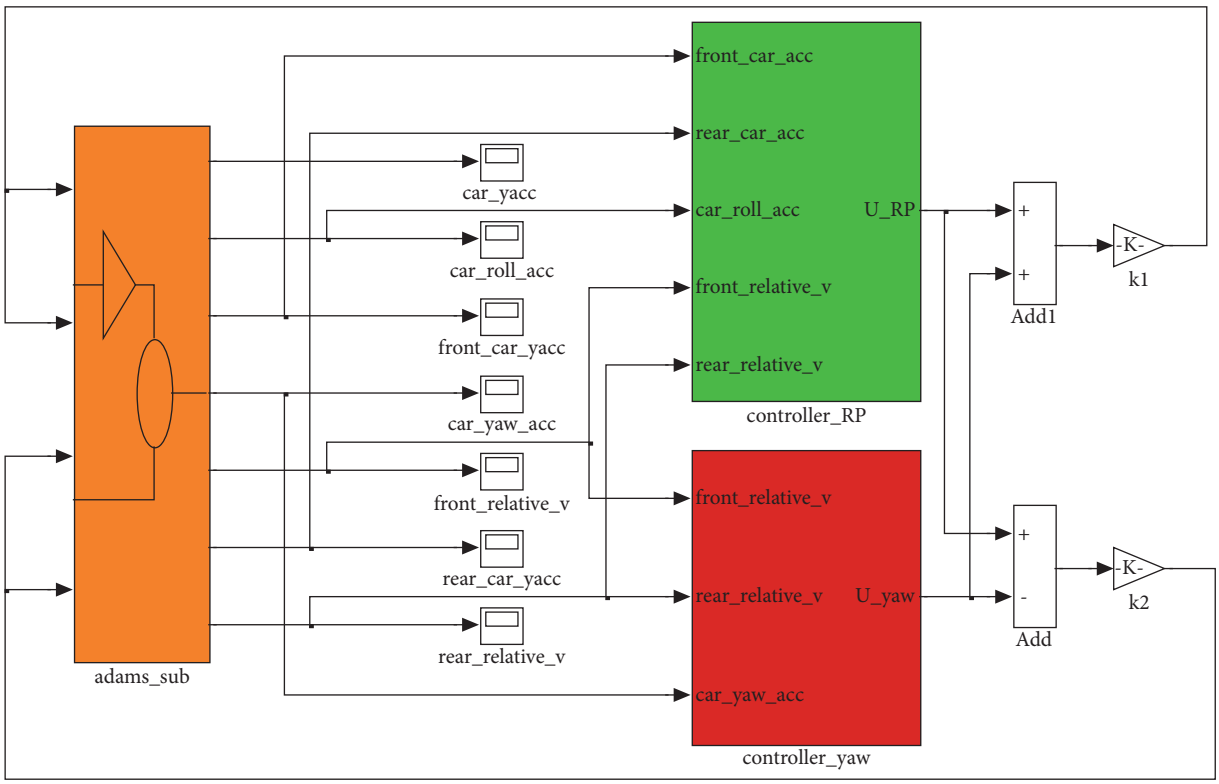

Figure 2: Robust nonfragile H_∞ controller of lateral semiactive suspension system of rail vehicle.

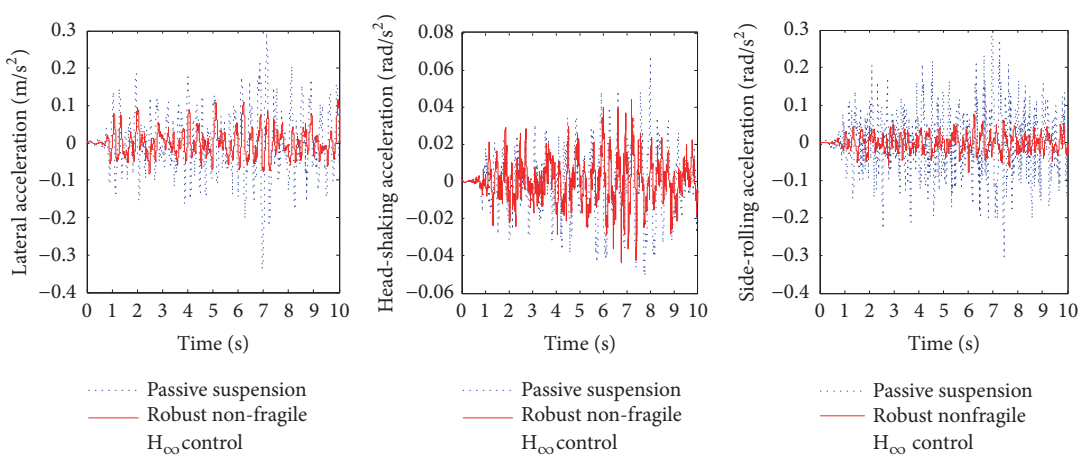

Figure 3: Acceleration time domain diagram. (a) Lateral-moving vibration. (b) Head-shaking vibration. (c) Side-rolling vibration.

Table 1: Time domain analysis of the vehicle body lateral acceleration amplitude and Sperling value comparison.

	Item	Passive suspension	Robust non-fragile H_∞ control	Improvement rate
Lateral moving	Maximum acceleration (m/s^2)	0.2954	0.1441	51.22%
	Sperling value	1.7697	1.3896	21.48%
Head shaking	Maximum angle acceleration (rad/s^2)	0.0677	0.0438	35.30%
Side rolling	Maximum angle acceleration (rad/s^2)	0.2855	0.0780	72.68%

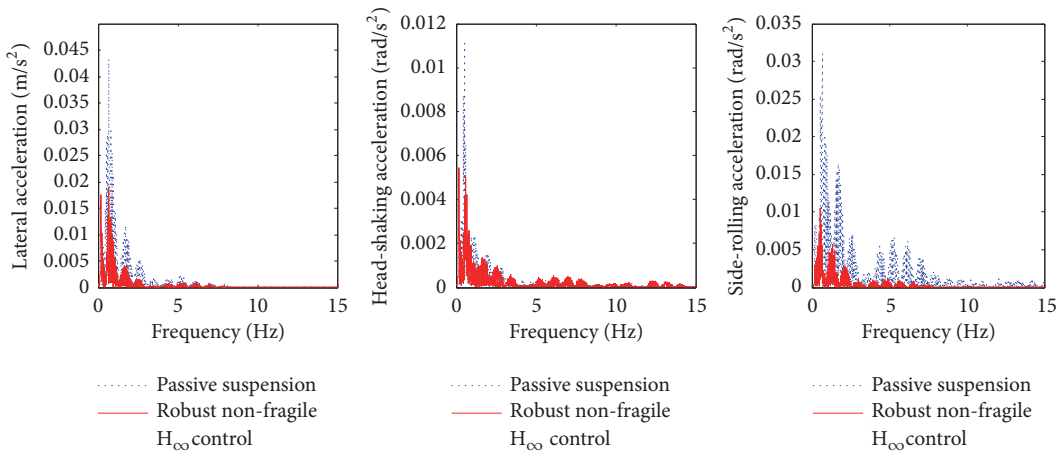

Figure 4: Acceleration frequency domain map. (a) Lateral-moving vibration. (b) Head-shaking vibration. (c) Side-rolling vibration.

Table 2: Comparison of the maximum acceleration of vehicle body in frequency domain analysis.

	Passive suspension	Robust non-fragile H_∞ control	Improvement rate
Lateral moving vibration acceleration (m/s^2)	0.0434	0.0191	55.99%
Head-shaking acceleration (rad/s^2)	0.0111	0.0054	51.35%
Side-rolling vibration acceleration (rad/s^2)	0.0311	0.0106	65.92%

Table 3: Acceleration power spectral density maximum contrast.

	Passive	Robust non-fragile H_∞ control	Reduction rate
Lateral-moving vibration PSD (m^2/s^3)	0.0044	0.0019	56.82%
Head-shaking PSD (rad^2/s^3)	0.0011	0.0006	45.45%
Side-rolling vibration PSD (rad^2/s^3)	0.0032	0.0011	65.63%

the comparison of Sperling comfort index and the amplitude of the time-domain analysis vehicle lateral damping accelerated speed. We can see from Table 1 that after adopting robust nonfragile H_∞ controller, compared with passive suspension, the maximums of accelerated speed of lateral-moving, head-shaking, and side-rolling vibration reduce by 51.22%, 35.30%, and 72.68%, respectively; and the Sperling value of accelerated speed of lateral-moving reduces by 21.48%.

4.2. Frequency Domain Analysis. Figure 4 shows the lateral vibration acceleration of the vehicle body in the two cases of passive suspension and robust nonfragile H_∞ control, respectively. It can be seen from Figure 4 that the body lateral-moving, head-shaking, and side-rolling vibration acceleration which are mainly concentrated in the 0~5Hz, compared with the passive suspension, are significantly improved in the frequency range after the use of robust nonfragile H_∞ control.

The comparison of the frequency domain analysis acceleration maximum values is shown in Table 2. It can be seen from Table 2 that the maximum nonfragile H_∞ control lateral-moving, head-shaking, and side-rolling vibration acceleration are $0.0191 m/s^2$, $0.0054 rad/s^2$, and $0.0106 rad/s^2$, respectively. Compared with the control effect of passive suspension, it can be seen that the maximum accelerations are reduced by 55.99%, 51.35%, and 65.92%, respectively.

The results of the analysis of the power spectral density (PSD) of the lateral-moving, head-shaking, and side-rolling of the rail vehicle are shown in Figure 5. The results of the analysis of the maximum power spectral density are shown in Table 3.

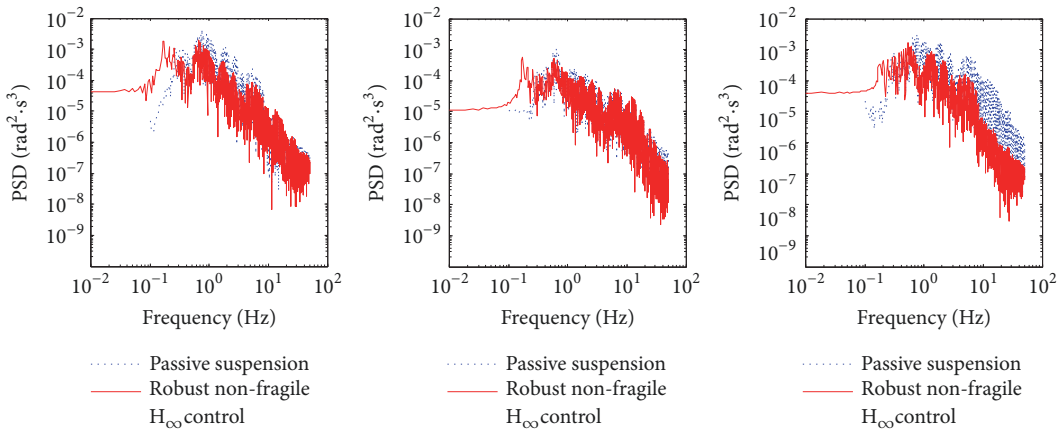

Figure 5: Comparison result of power spectrum. (a) Lateral-moving vibration. (b) Head-shaking vibration. (c) Side-rolling vibration.

Table 4: Vehicle body head-shaking acceleration zero pole value.

Controller gain	Conventional robust H_∞ Control		Robust non-fragile H_∞ control	
	Zero point z	Pole p	Zero point z	Pole p
Without perturbation	-6.7296	-1.8805+4.6662i	-3.7942	-13.7740
	0.0000	-1.8805-4.6662i	0.0000	-1.0360
With perturbation	-7.8835	0.2894 +5.4375i	-4.9482	-8.5680
	0.0000	0.2894 - 5.4375i	0.0000	-2.1720

Table 5: Vehicle body vibration acceleration zero pole value.

Controller gain	Conventional robust H_∞ Control		Robust non-fragile H_∞ control	
	Zero point z	Pole p	Zero point z	Pole p
Without perturbation	-2.1322 + 8.9026i	-32.5642	-1.1022 + 8.9834i	-40.0488
	-2.1322 - 8.9026i	-2.1884 + 8.7767i	-1.1022 - 8.9834i	-0.6795 + 8.9088i
	-0.6741	-2.1884 -8.7767i	-0.9034	-0.6795 - 8.9088i
	0.0000	-0.6891	0.0000	-0.7523
With perturbation	-6.3286 + 7.7512i	-8.6896+22.3172i	-5.3252 + 8.1739i	-10.2541+18.6985i
	-6.3286 - 7.7512i	-8.6896 -22.3172i	-5.3252 - 8.1739i	-10.2541 -18.6985i
	0.1587	-1.9441	-0.0172	-2.8406
	0.0000	0.4633	0.0000	-0.0412

It can be seen from Figure 5 that the acceleration power spectral density function of the lateral-moving vibration, side-rolling vibration, and head-shaking vibration of the rail vehicle is mostly distributed in the low frequency range. According to the data of Table 3, it can be seen that for the passive suspension, lateral-moving, head-shaking, and side-rolling vibration acceleration reach the maximum values at 0.7532, 0.6433, and 0.7532Hz, respectively, and the maximum values are 0.0044m^2/s^3, 0.0011rad^2/s, and 0.0032rad^2/s^3; for robust nonfragile H_∞ control, the accelerations of the lateral-moving, head-shaking, and side-rolling vibration after control reach 0.6532, 0.1709, and 0.5311Hz, and the maximum values of acceleration are 0.0019m^2/s^3, 0.0006rad^2/s^3, and 0.0011rad^2/s^3. The maximum values of the acceleration power spectral density of the robust nonfragile H_∞ control are 56.82%, 45.45%, and 65.63% lower than that of the passive suspension, respectively.

4.3. Controller Fragility Analysis. In order to verify the non-fragility of the semiactive control suspension system, the step responses of the simultaneously existing gain perturbations of the robust nonfragile H_∞ controller and the conventional robust H_∞ controller are studied by zero-pole analysis. Figures 6–11 are zero-pole distribution maps of transfer function of vehicle body head-shaking and side-rolling control system when gain perturbation arises or does not arise in controller. Tables 4–6 are zero-pore values of transfer function of vehicle body head-shaking and side-rolling control system, when gain perturbation arises or does not arise in controller.

It can be seen from Figures 6 and 7 and Table 4 that as for the vehicle body head-shaking controller when there is no controller gain perturbation the two poles of the robust nonfragile H_∞ controller and the conventional robust H_∞ controller are distributed in the left planes, and the controller is stable.

Table 6: Vehicle body vibration acceleration zero pole value.

Controller gain	Conventional robust H_∞ Control		Robust non-fragile H_∞ control	
	Zero point z	Pole p	Zero point z	Pole p
Without perturbation	-6.4136	-32.5642	52.6622	-40.0488
	0.0004	-2.1884 + 8.7767i	-0.0190	-0.6795 + 8.9088i
	0.0001	-2.1884 - 8.7767i	0.0000	-0.6795 - 8.9088i
	-0.0001	-0.6891	0.0000	-0.7523
With perturbation	-250.8154	-8.6896+22.3172i	-191.76	-10.2541 +18.6985i
	-0.0164	-8.6896 -22.3172i	-0.0200	-10.2541 -18.6985i
	-0.0000	-1.9441	0.0000	-2.8406
	0.0000	0.4633	0.0000	-0.0412

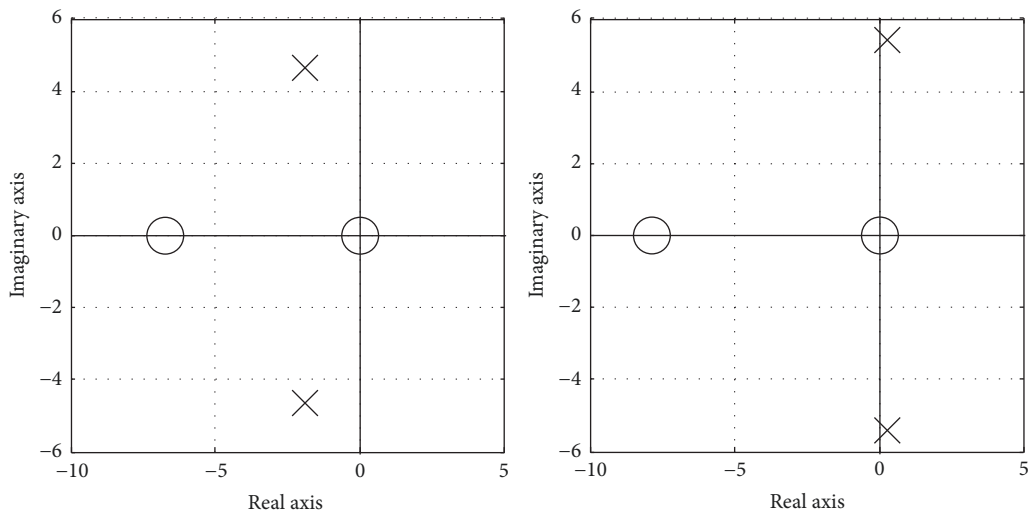

Figure 6: Conventional robust H_∞ control for vehicle body head-shaking acceleration. (a) Without perturbation. (b) With perturbation.

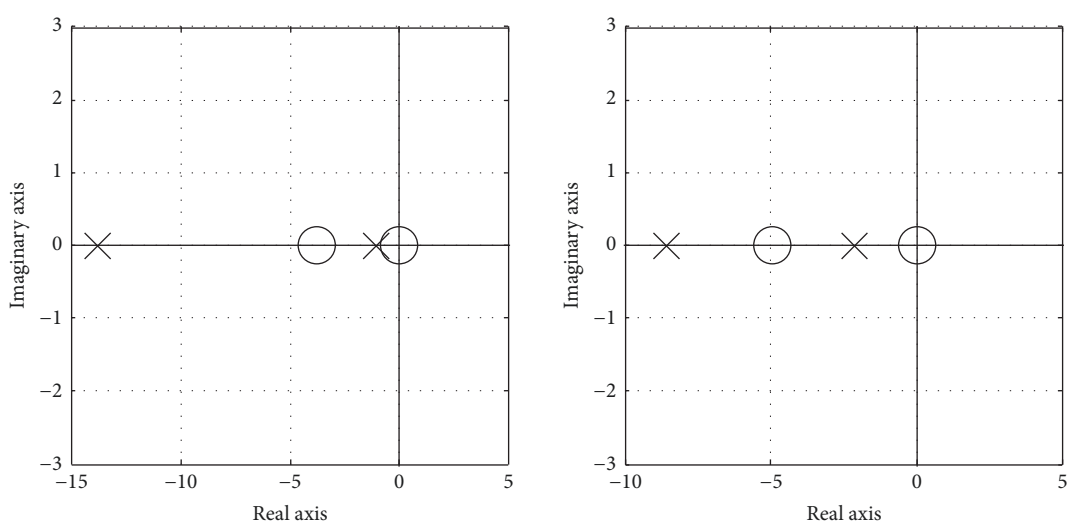

Figure 7: Robust nonfragile H_∞ control for vehicle body head-shaking acceleration. (a) Without perturbation. (b) With perturbation.

When gain perturbation arises in controller, the two poles of the robust nonfragile H_∞ controller are distributed in the left plane gain perturbation left half plane, while the two poles of the conventional robust H_∞ controller are distributed in the right planes and the controller is unstable.

From Figures 10 and 11 and Tables 4–6, it can be seen that for the rolling motion control of the body roll movement controller, when no gain perturbation arises in controller, the total four poles of nonfragile H_∞ controller and the conventional robust H_∞ controller are distributed in the left

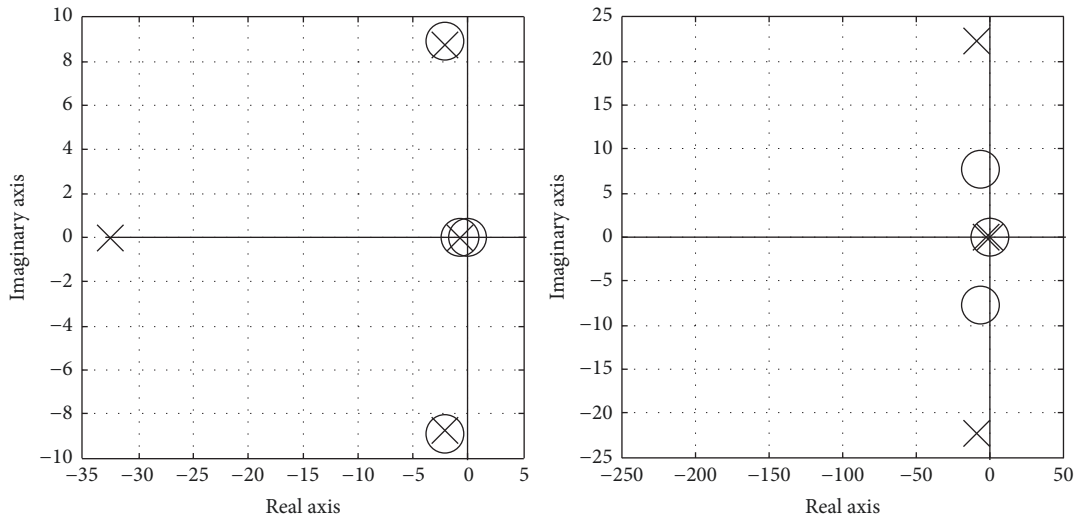

Figure 8: Conventional robust H_∞ control for vehicle body lateral acceleration. (a) Without perturbation. (b) With perturbation.

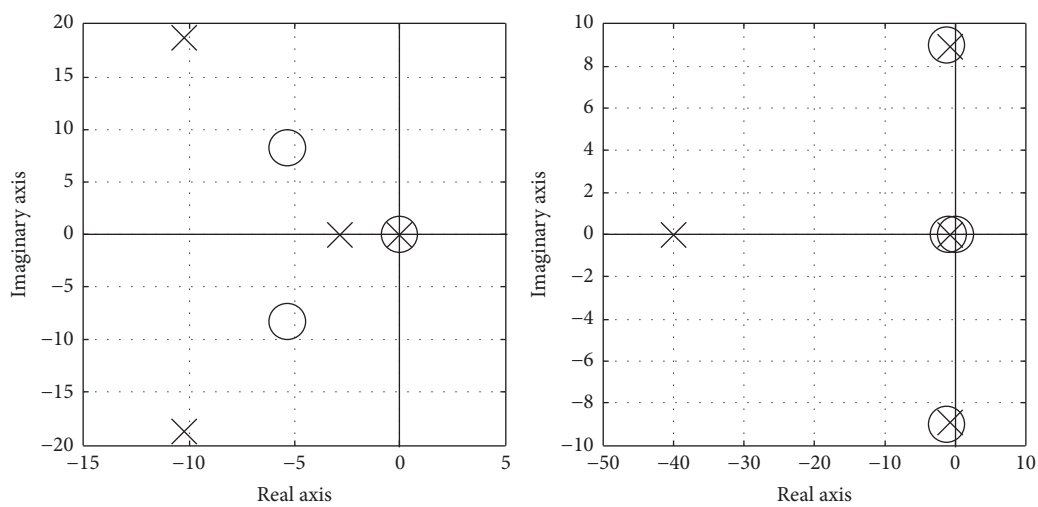

Figure 9: Robust H_∞ nonfragile control for vehicle body lateral acceleration. (a) Without perturbation. (b) With perturbation.

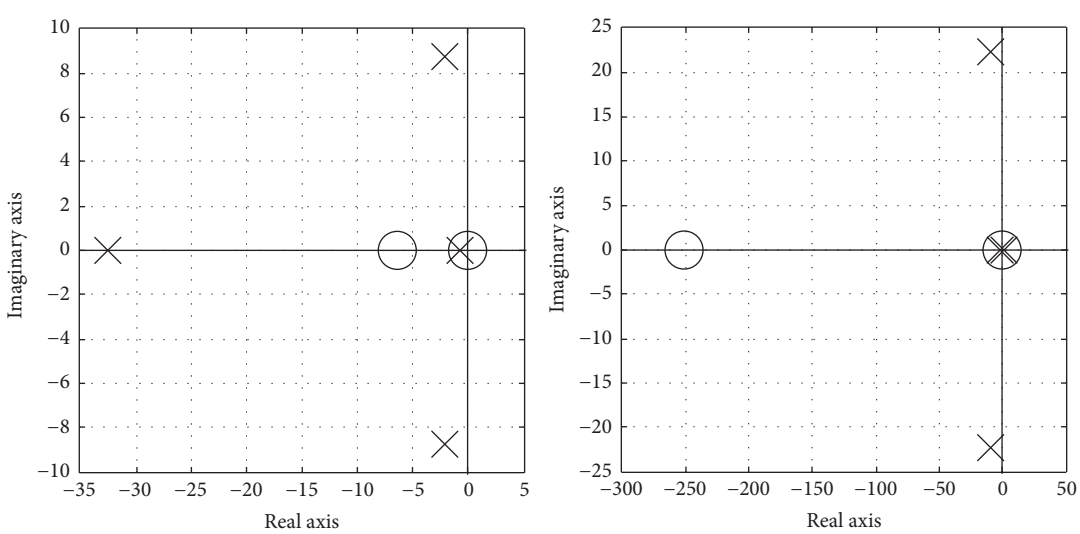

Figure 10: Conventional robust H_∞ control for vehicle body side-rolling acceleration. (a) Without perturbation. (b) With perturbation.

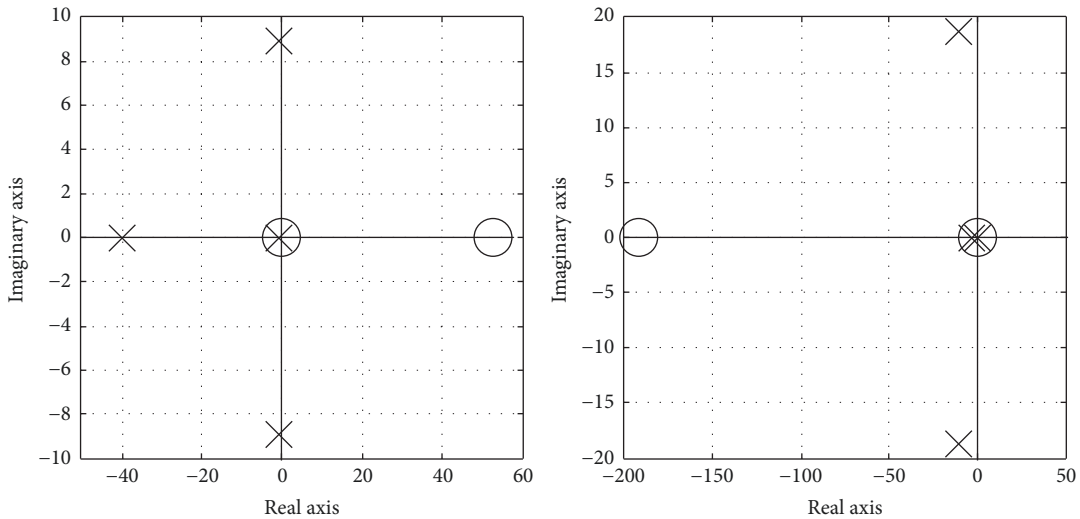

Figure 11: Robust H∞ nonfragile control for vehicle body side-rolling acceleration. (a) Without perturbation. (b) With perturbation.

half planes, and the controller is stable; when the controller gain perturbations occur, the four poles of robust and nonfragile H_∞ controllers are located in the left planes, and the controller is stable, while when a pole of the conventional H_∞ controller locates in the right planes, the controller is unstable.

5. Conclusion

In this paper, the lateral semiactive suspension control model of the rail vehicle is established firstly, then the robust nonfragile H_∞ controller of the vehicle body head-shaking vibration and the body rolling motion are established by taking full account of the gain perturbation of the controller, and the linear matrix inequality is taken to solve the problems. In this paper, the passive control, conventional robust H_∞ control, and the robust nonfragile H_∞ control established in this paper are compared and analyzed by using ADAMS and MATLAB joint simulation in German low-interference track spectrum. The results of simulation show that compared with the passive control, the robust nonfragile H_∞ controller designed in this paper can effectively restrain the lateral-moving, head-shaking, and side-rolling of the vehicle body and effectively guarantee the riding comfort of the vehicle. When gains arise out of a controller, compared with the conventional H_∞ robust controller, the robust nonfragile H_∞ controller designed in this paper can still maintain its good performance and a comparatively strong nonvulnerability. The results of this paper are based on the linear matrix inequality (LMI) 2 technology, so nonconvex matrix inequality (nonlinear coupling) conditions will be encountered in further research [18].

Data Availability

The data used to support the findings of this study are included within the article.

Conflicts of Interest

No potential conflict of interest was reported by the authors.

Acknowledgments

This work was supported by the National Natural Science Foundation of China (NSFC) [61563027] and Lzjtu (201604) EP Support under Grants.

References

[1] Z. Q. Yang, J. M. Zhang, and Z. C. Chen, "Semi-active control of high-speed trains based on fuzzy PID control," *Procedia Engineering*, vol. 15, no. 1, pp. 2163–2167, 2011.

[2] W. S. Ding, J. L. Bu, and Y. M. Liu, "Strategy and method of high-speed train suspension's lateral semi-active control in China," *China Railway Science*, vol. 23, no. 4, pp. 1–7, 2002.

[3] C. Hsieh, B. Huang, F. Golnaraghi, and M. Moallem, "Regenerative Skyhook Control for an Electromechanical Suspension System Using a Switch-Mode Rectifier," *IEEE Transactions on Vehicular Technology*, vol. 65, no. 42, pp. 9642–9650, 2016.

[4] J. Guo, Z. Xu, and Y. Sun, "A new semi-active safety control strategy for high-speed railway vehicles," *Vehicle System Dynamics*, vol. 53, no. 12, pp. 1918–1934, 2016.

[5] S. Chen, R. He, and H. Liu, "An optimal design for suspension based on LQG control," in *Electric Information and Control Engineering*, pp. 1987–1992, 2011.

[6] M. Sunwoo, K. Cheok, and N. Huang, "Model reference adaptive control for vehicle active suspension systems," *IEEE Transactions on Industrial Electronics*, vol. 38, no. 3, pp. 217–222, 1991.

[7] K.-H. Guo, J.-K. Sui, and Y.-H. Guo, "Semi-active control method for a high-speed railway vehicle lateral damper based on skyhook and groundhook hybrid damping," *Journal of Vibration & Shock*, vol. 32, no. 2, pp. 18–23, 2012.

[8] H. Y. Liu, J. Zeng, and L. Li, "Study on secondary lateral continuous adjustable damping semi-active suspension device for high-speed train," *China Railway Science*, vol. 33, no. 4, pp. 69–74, 2012.

[9] G.-J. Li, W.-D. Jin, and C.-J. Chen, "Variable universe fuzzy control of train lateral semi-active suspension system," *Optics and Precision Engineering*, vol. 21, no. 12, pp. 3298–3307, 2013.

[10] Z. J. Zhong, H. Y. Dai, and J. Zeng, "Fuzzy semi-active control of railway vehicle with magnetorheological dampers," *Journal of Traffic and Transportation Engineering*, vol. 25, no. 5, pp. 43–50, 2014.

[11] L. H. Keel and S. P. Bhattacharyya, "Robust, fragile, or optimal," *IEEE Trans on Automatic Control*, vol. 42, no. 8, pp. 1098–1105, 1997.

[12] B.-L. Zhang, Z.-W. Huang, and Q.-L. Han, "Delayed non-fragile H∞ control for offshore steel jacket platforms," *Journal of Vibration and Control*, vol. 21, no. 1, pp. 959–974, 2015.

[13] S. B. Liu, D. X. Zhao, and T. Shang, "Non-fragile H2/ generalized H2 optimal control for active suspension based on static output feedback," *Journal of Sichuan University Engineering*, vol. 43, no. 1, pp. 240–246, 2011.

[14] Y. X. Kong, D. X. Zhao, B. Yang, C. H. Han, and J. Y. Han, "Non-fragile H∞/ L2- L∞Static Output Feedback Control of Active Suspension with Actuator Input Delay," *Transactions of the Chinese Society of Agricultural Machinery*, vol. 8, pp. 1–7, 2014.

[15] Y. P. Lan and W. He, "Non-fragile robust controller design for magnetic levitation permanent magnet linear motor," *Manufacturing Technology & Machine Tool*, vol. 15, no. 9, pp. 80–83, 2013.

[16] L. Yu, *Robust Control-Linear Matrix Inequality Processing*, Tsinghua University Press, 2002.

[17] L.-H. Zong, X.-L. Gong, S.-H. Xuan, and C.-Y. Guo, "Semi-active H∞ control of high-speed railway vehicle suspension with magnetorheological dampers," *Vehicle System Dynamics*, vol. 51, no. 5, pp. 600–626, 2013.

[18] X. Chang and G. Yang, "New results on output feedback H∞ control for linear discrete-time systems," *IEEE Transactions on Automatic Control*, vol. 59, no. 5, pp. 1355–1359, 2014.